Vibrational excitations in a-$Si_{1-x}Ge_x$:F, a-$Si_{1-x}Ge_x$:H, and $Ga_{1-x}Al_xAs$ alloys

Bal K. Agrawal, B. K. Ghosh, and P. S. Yadav
Department of Physics, University of Allahabad, Allahabad 211 002, Uttar Pradesh, India
(Received 18 December 1986; revised manuscript received 21 January 1988)

We report here the results of a *first* calculation of the vibrational excitations of hydrogenated (or fluorinated) a-$Si_{1-x}Ge_x$:H (a-$Si_{1-x}Ge_x$:F) and the unhydrogenated $Ga_{1-x}Al_xAs$ alloys using a cluster Bethe-lattice method. The study has been made for two types of distributions of constituent atoms of the alloy: a random sequence and a chemically ordered one. The Raman data of a-$Si_{1-x}Ge_x$ alloys can be well understood if one assumes the occurrence of a chemically ordered sequence in which every minority atom has majority atoms located at all nearest-neighboring sites. The vibrational modes induced by H (F) atoms outside the bulk phonon region of an a-$Si_{1-x}Ge_x$ alloy remain undisturbed by the presence of the kind of atoms lying on the next-nearest-neighboring sites of the H (F) atom. On the other hand, the frequencies of modes induced by F atoms lying in the bulk phonon region change regularly due to the different concentrations of the Si and Ge atoms in the alloy. The calculated results are in good agreement with the available infrared and Raman data. However, more careful and detailed experimental investigations are very much needed to detect the predicted extra structure especially in the bulk phonon-frequency region. For $Ga_{1-x}Al_xAs$ alloys, the two-mode behavior is very clearly evident in the calculated local phonon density of states. The available experimental data in the optical-phonon region is in excellent agreement with the computed phonon density for $Ga_{1-x}Al_xAs$ alloys, under assumption of a random distribution of Ga and Al atoms.

I. INTRODUCTION

Improvement in the conversion efficiency is the most important point for the practical application of the a-Si solar cell as an alternate nonconventional source of energy. A conversion efficiency of 11–12 % has recently been reached in Si-based devices in textured structures.[1] In an attempt to attain much higher conversion efficiency, multiple-band-gap a-Si solar cells have to be developed. This attempt stems from the fact that in contrast to the theoretical limit of maximum efficiency of 12.5–13 % for the conventional single-band-gap a-Si solar cell, multiple-band-gap a-Si solar cells, named tandem solar cells, may have an estimated value of 21–24 %.[2]

Amorphous hydrogenated or fluorinated silicon germanium alloys have an energy gap smaller than that of a-Si:H or a-Si:F,H. They have potential applications in tandem solar cells and also in electrophotography. Numerous experimental investigations have so far been reported in the literature.[3]

GaAs is a direct-band-gap material and can thus sustain much faster electrons as compared to those in silicon. The various properties of GaAs alloys are thus opening the way for new electronic devices, including logic circuits which can operate at much higher speeds, microwave devices that can operate at higher frequencies, and circuits that interface easily with optical fibers.

Along with the electrical properties, Paul[4] also measured the infrared vibrational absorption spectra of a-$Si_{1-x}Ge_x$:H alloys on the samples prepared by glow discharge decomposition of gas mixtures. Peaks corresponding to the Si:H and Ge:H stretching vibrations were detected by these authors using a dual magnetron sputtering technique. Rudder *et al.*[5] have reported the results of infrared transmission measurements on a-$Si_{0.47}Ge_{0.53}$ samples containing H atoms. These authors have suggested the occurrence of dihydrides in these alloys. Very recently Tsuda *et al.*[6] have fabricated very good quality a-Si-Ge:H,F films by glow charge and measured the Raman spectra of the alloys in the frequency region 200–550 cm^{-1}. They detected peaks arising mainly from the Si—Si, Si—Ge, and Ge—Ge bonds.

In contrast to the many experimental investigations, virtually no theoretical attempt has been made to understand the behavior of the hydrogenated or fluorinated semiconducting alloys. In particular, no result of any serious investigation of the hydrogenated and/or fluorinated amorphous $Si_{1-x}Ge_x$, $Si_{1-x}C_x$, or $Si_{1-x}N_x$ alloy has so far been reported. In fact, for *pure* Si_xGe_{1-x} alloys, some calculations[7–10] have been reported. Our group is presently engaged in a detailed theoretical study of the vibrational and electronic excitations of these semiconducting alloys containing H, F, O, etc. The present article is the second of a series of our reports on these materials. The results for the electronic structure of a-$Si_{1-x}Ge_x$:F,H alloys has already been reported.[11]

Earlier, Agrawal[9] had investigated the vibrational structures of the Si_xGe_{1-x} alloys using a five-atom cluster Bethe-lattice method (CBLM) and reported the results for the different probabilistic arrangements of the constituent atoms in these alloys.

Special interest has recently been shown[12] in the study of the compositional dependence of the optical-phonon frequencies of the $Ga_{1-x}Al_xAs$ system because the lattice mismatch between the two end compounds, GaAs and AlAs, is extremely small. Thus, the substitutional solid

solutions can be taken to be ideal and nearly free of mechanical stress. This results in an essentially random distribution of Ga and Al ions in these alloys and causes little or no fine structure in the reflectance spectra which could have arisen from a probable microscopic scale clustering of like atoms. On the other hand, the replacement of the Ga atoms increases the fundamental electron energy gap parameter with the concentration of the added Al atoms. This facility has already been exploited in achieving modulation doping where the in-plane electron and hole mobilities are enhanced by several orders of magnitude in GaAs/$Ga_{1-x}Al_xAs$ superlattices.

An understanding of the elementary excitations like phonons and electrons in $Ga_{1-x}Al_xAs$ alloys in bulk is imperative before a complete knowledge of the various properties of the GaAs/$Ga_{1-x}Al_xAs$ heterojunctions is achieved.

A cluster Bethe-lattice method is particularly suited for the study of short-range order to disorder. The usefulness of the method arises from the fact that the properties of small regions of atoms can be isolated. Here, the problem is exactly solvable in contrast to the difficulties faced in other methods.

In the present article, we report the results of our investigations of the phonons of the hydrogenated and/or fluorinated amorphous $Si_{1-x}Ge_x$ alloys and of the unhydrogenated (unfluorinated) $Ga_{1-x}Al_xAs$ alloys. The Raman data of a-$Si_{1-x}Ge_x$ alloys can be well understood if one assumes the occurrence of a chemically ordered sequence in which every minority atom has majority atoms as all its neighbors. The calculated local phonon density of states for the various concentrations of Al atoms in GaAs alloys is seen to be in excellent agreement with the only available data for the reflectivity spectra and a two-mode behavior is very clearly evident in the local phonon density of states. Section II contains a brief account of the cluster Bethe-lattice method used for the alloys along with the interpolation scheme for relating the bond probabilities to the branching ratios of a Cayley tree. The results of the numerical calculations for the phonons of the a-$Si_{1-x}Ge_x$:H and the a-$Si_{1-x}Ge_x$:F alloys are contained in Sec. III. Section IV includes the results for the $Ga_{1-x}Al_xAs$ alloys and the main conclusions are given in Sec. V.

II. THEORY

A. Cluster Bethe-lattice method

The cluster Bethe-lattice method involves treating a part of an infinitely connected network of atoms exactly as a cluster and representing the effect of the rest of the environment by connecting the Bethe lattice to the surface of the cluster. The Bethe lattice is an infinite network of atoms with the appropriate coordination number devoid of any ring structure. It provides a natural background upon which the individual properties of the cluster are studied.

For a dynamical or Hamiltonian matrix describing the system, the local Green's function $\underline{G}$ of the central atom can be obtained exactly. In the Bethe-lattice one preserves the connectivity of the system. Also, the density of the energy states of the Bethe lattice is smooth and featureless and therefore, the effects of the local environment of the reference atom appear in its local state density.

The Green's function (GF) for a system may be defined as

$$\underline{G}=(\omega^2\underline{I}-\underline{D})^{-1}\ , \tag{1}$$

and one may expand it in the form of Dyson equation as

$$(\omega^2\underline{I}-\underline{D}^0)\underline{G}=\underline{I}+\underline{V}\underline{G}\ ,$$

where

$$\underline{D}=\underline{D}^0+\underline{V}\ . \tag{2}$$

Here $\underline{D}^0$ and $\underline{V}$ are the diagonal and the nondiagonal parts of the mass-reduced dynamical matrix $\underline{D}$, $\underline{I}$ is the unit matrix, and ω is the phonon frequency. For electrons, the dynamical matrix $\underline{D}$ is replaced by the full Hamiltonian of the system and ω^2 by E, the electron energy.

Once $\underline{G}$ is known, various properties of the system can be calculated. The density of states, i.e., the fractional number of states lying between ω^2 and $\omega^2+d\omega^2$ of the system is given by

$$N(\omega^2)=-(1/\pi)\mathrm{Im}\,|\,\mathrm{Tr}\underline{G}(\omega^2)\,|\ . \tag{3a}$$

Equivalently, the fractional number of states lying between ω and $\omega+d\omega$, i.e., the usual density of states, is given by

$$N(\omega)=-(2\omega/\pi)\mathrm{Im}\,|\,\mathrm{Tr}\underline{G}(\omega^2)\,|\ . \tag{3b}$$

One is, therefore, interested in the diagonal matrix element of $\underline{G}(\omega^2)$. The matrix element of $G(\omega^2)$ for a basis $|\,i\,\rangle$, are given by

$$\omega^2\langle i\,|\,\underline{G}(\omega^2)\,|\,j\,\rangle=\underline{I}_{ij}+\sum_{k=1}^{4}\langle i\,|\,\underline{V}\,|\,k\,\rangle\langle k\,|\,\underline{G}\,|\,j\,\rangle\ . \tag{4}$$

The local Green's function of the ith atom can then be computed by determining $\langle i\,|\,\underline{G}\,|\,i\,\rangle$ and the local density of states at the ith atom by

$$N_i(\omega^2)=(-1/\pi)\mathrm{Im}\,|\,\mathrm{Tr}\langle i\,|\,\underline{G}\,|\,i\,\rangle\,|\ , \tag{5}$$

where Im Tr denotes the imaginary part of the trace of matrix.

The infinite set of coupled equations (4) can be reduced to a finite set with the help of the symmetries of the Bethe lattice using the transfer matrices or the effective fields. In the ringless structure of the Bethe lattice, every Green's-function matrix element can be transformed to another one by a fixed set of transformations.

The Green's-function matrix elements between two atoms (i,k) having larger separation in the Bethe lattice are related to that between two atoms (i,j) lying close to each other by

$$\underline{G}_{ki}=\underline{t}_{kj}\underline{G}_{ji}\ . \tag{6}$$

Here $\underline{t}_{kj}$ is the transfer matrix or effective field at site k along the direction of the atom j. By definition, the same

site GF at one site should be equivalent to one at another site. We may thus write the local Green's-function matrix element for site i as

$$\underline{G}_{ii}=(\omega^2\underline{I}-\underline{D}^{0}_{ii}-\underline{F})^{-1}\ , \tag{7}$$

where

$$\underline{F}=\sum_j \underline{V}_{ij}\underline{t}_{ji}\ . \tag{8}$$

B. A_xB_{1-x} alloys

In binary A_xB_{1-x} alloys, there are various probabilities of the occurrence of the A—A, A—B, B—A, and B—B bonds. We consider a reference site in the Cayley tree. The descendants of this reference site will be determined by the level of the valence saturation already present due to its parent atom. For an alloy having the same coordination for the two kinds of atoms, e.g., the Si_xGe_{1-x} alloy, let us assume that P_a (Q_a) is the probability of like (unlike) atom descendants of an A atom. The branching ratios of the descendants would be consistent with the saturation condition and the cluster averages for the different values of average probabilities. We consider the following three different sequences for describing the different bonding tendencies.

a. Random sequence. In this sequence, each kind of atom has an equal probability of saturating the valence of an atom compatible with the equal multiplicities. The probability of the occurrence of an atom is directly proportional to its concentration in the alloy. Thus, for a concentration x of atoms of kind A, one may write

$$\begin{aligned} &P_a=x,\quad Q_a=1-x\ ,\\ &P_b=1-x,\quad Q_b=x\ . \end{aligned} \tag{9}$$

b. Chemically ordered sequence. In this sequence, atoms in small concentration are likely to be surrounded by the atoms in high concentration. For small concentration x ($x<0.5$) of atoms A, we may write

$$\begin{aligned} &P_a=0,\quad Q_a=1\ ,\\ &P_b=(1-2x)/(1-x),\quad Q_b=x/(1-x)\ . \end{aligned} \tag{10}$$

In the case where the B atoms are present in low concentration, x will be replaced by $1-x$ in the above expressions.

c. Segregation sequence. In some alloys it is observed that like atoms cluster. This will result in the absence of any bond between unlike atoms, i.e., there are no A—B, B—A bonds. The probabilities are then given by

$$\begin{aligned} &P_a=P_b=1\ ,\\ &Q_a=Q_b=0\ . \end{aligned} \tag{11}$$

In a binary alloy A_xB_{1-x}, a particular kind of atom can have both kinds of neighbors. One needs to know the two different effective fields (transfer matrices) for each kind of reference atom. For the reference atom A, one will have the transfer matrices t_{aa} and t_{ab}. Similarly, for the reference atom B, we should know t_{ba} and t_{bb}. Thus for every lattice site there are four unknown types of the transfer matrices. For a nearest-neighboring site of the reference atom, we will similarly have four transfer matrices named

$$\bar{t}_{aa},\ \bar{t}_{ab},\ \bar{t}_{ba}\ \text{ and }\ \bar{t}_{bb}\ .$$

The above unknown eight kinds of transfer matrices are related among themselves by the following self-consistent equations:

$$\begin{aligned}
\underline{t}^{\,i}_{aa}&=\left[\omega^2\underline{I}-\underline{D}^{0}_{aa}-P_a\sum_k{}'\,\underline{V}^{k\,T}_{aa}\underline{\bar{t}}^{\,k}_{aa}-Q_a\sum_k{}'\underline{V}^{k\,T}_{ab}\underline{\bar{t}}^{\,k}_{ab}\right]^{-1}\underline{V}^{i\,T}_{aa}\ ,\\
\underline{\bar{t}}^{\,i}_{aa}&=\left[\omega^2\underline{I}-\underline{D}^{0}_{aa}-P_a\sum_j{}'\,\underline{V}^{j}_{aa}\underline{t}^{\,j}_{aa}-Q_a\sum_j{}'\underline{V}^{j}_{ab}\underline{t}^{\,j}_{ab}\right]^{-1}\underline{V}^{i}_{aa}\ ,\\
\underline{t}^{\,i}_{ab}&=\left[\omega^2\underline{I}-\underline{D}^{0}_{bb}-P_b\sum_k{}'\,\underline{V}^{k\,T}_{bb}\underline{\bar{t}}^{\,k}_{bb}-Q_b\sum_k{}'\underline{V}^{k\,T}_{ba}\underline{\bar{t}}^{\,k}_{ba}\right]^{-1}\underline{V}^{i\,T}_{ba}\ ,\\
\underline{\bar{t}}^{\,i}_{ab}&=\left[\omega^2\underline{I}-\underline{D}^{0}_{bb}-P_b\sum_j{}'\,\underline{V}^{j}_{bb}\underline{t}^{\,j}_{bb}-Q_b\sum_j{}'\underline{V}^{j}_{ba}\underline{t}^{\,j}_{ba}\right]^{-1}\underline{V}^{i}_{ba}\ ,\\
\underline{t}^{\,i}_{bb}&=\left[\omega^2\underline{I}-\underline{D}^{0}_{bb}-P_b\sum_k{}'\,\underline{V}^{k\,T}_{bb}\underline{\bar{t}}^{\,k}_{bb}-Q_b\sum_k{}'\underline{V}^{k\,T}_{ba}\underline{\bar{t}}^{\,k}_{ba}\right]^{-1}\underline{V}^{i\,T}_{bb}\ ,\\
\underline{\bar{t}}^{\,i}_{bb}&=\left[\omega^2\underline{I}-\underline{D}^{0}_{bb}-P_b\sum_j{}'\,\underline{V}^{j}_{bb}\underline{t}^{\,j}_{bb}-Q_b\sum_j{}'\underline{V}^{j}_{ba}\underline{t}^{\,j}_{ba}\right]^{-1}\underline{V}^{i}_{bb}\ ,\\
\underline{t}^{\,i}_{ba}&=\left[\omega^2\underline{I}-\underline{D}^{0}_{aa}-P_a\sum_k{}'\,\underline{V}^{k\,T}_{aa}\underline{\bar{t}}^{\,k}_{aa}-Q_a\sum_k{}'\underline{V}^{k\,T}_{ab}\underline{\bar{t}}^{\,k}_{ab}\right]^{-1}\underline{V}^{i\,T}_{ab}\ ,\\
\underline{\bar{t}}^{\,i}_{ba}&=\left[\omega^2\underline{I}-\underline{D}^{0}_{aa}-P_a\sum_j{}'\,\underline{V}^{j}_{aa}\underline{t}^{\,j}_{aa}-Q_a\sum_j{}'\underline{V}^{j}_{ab}\underline{t}^{\,j}_{ab}\right]^{-1}\underline{V}^{i}_{ab}\ .
\end{aligned} \tag{12}$$

Here, $\underline{t}^{i}_{aa}$ ($\underline{\bar{t}}^{i}_{aa}$), $\underline{t}^{i}_{ab}$ ($\underline{\bar{t}}^{i}_{ab}$), $\underline{t}^{i}_{ba}$ ($\underline{\bar{t}}^{i}_{ba}$), and $\underline{t}^{i}_{bb}$ ($\underline{\bar{t}}^{i}_{bb}$) are the transfer matrices along the A—A, A—B, B—A, and B—B bonds, respectively, in the direction i. $\sum'$ denotes summation over all the nearest neighbors of an atom except the one in the direction i, and $\underline{V}^{T}$ is the transpose matrix of $\underline{V}$.

The local Green's functions at A and B atoms are, respectively,

$$\underline{G}_{aa}=\left[\omega^2\underline{I}-\underline{D}^{0}_{aa}-P_a\sum_{j=1}^{4}\underline{V}^{j}_{aa}\underline{t}^{j}_{aa}-Q_a\sum_{j=1}^{4}\underline{V}^{j}_{ab}\underline{t}^{j}_{ab}\right]^{-1}, \tag{13}$$

$$\underline{G}_{bb}=\left[\omega^2\underline{I}-\underline{D}^{0}_{bb}-P_b\sum_{j=1}^{4}\underline{V}^{j}_{bb}\underline{t}^{j}_{bb}-Q_b\sum_{j=1}^{4}\underline{V}^{j}_{ba}\underline{t}^{j}_{ba}\right]^{-1}.$$

C. Valence force field model

For treating the vibrations of the clusters containing the alloying atoms like H and F, we employ the rotationally invariant valence force field model (VFFM). The potential energy in VFFM can be written as

$$V=\tfrac{3}{4}\alpha\sum_{l,l'}[(\mathbf{u}_l-\mathbf{u}_{l'})\cdot\mathbf{e}_{ll'}]^2+\tfrac{1}{2}\sum_{l,l'}K_{ll'}r_{0l}r_{0l'}(\Delta\phi_{l0l'})^2\,, \tag{14}$$

where the sums are over all the atoms l and their nearest neighbors l'. The first term represents the elastic energy due to changes in bond lengths. Here α is the radial force constant, $\mathbf{u}_l$'s are the atomic displacements of atom l, and $\mathbf{e}_{ll'}$, is the unit vector in the direction of the line joining the atoms l and l'.

The second term represents the energy arising from the changes in the bond angles $\Delta\phi_{l0l'}$, formed by the atoms l and l' at the reference atom 0. Here, r_{ij} is the bond length between the atoms i and j and K_{ll}'s are the angle bending force constants.

III. CALCULATION AND RESULTS

A. a-Ge_xSi_{1-x} alloys

The local phonon densities of states at both the Ge and Si atoms have been calculated for the entire concentration range ($0.01<x<0.99$) both for the random and chemically ordered sequences. The results for the two sequences are shown in Figs. 1 and 2, respectively. For the sake of comparison, the results for bulk Si and Ge matrices lying at the two ends of the alloy are also included. For a low concentration x of the Ge atoms in the silicon matrix, a peak arising from the Ge—Ge bonds appears at 205 cm^{-1}. The frequency of the other strong peak arising from the Si—Si TO-like modes decreases with increase in x. The large Ge—Ge bond mode shifts to higher frequency with x. For large values of x ($x>0.5$), the number of Ge—Ge bonds increases and the corresponding peak splits into two separate peaks; one peak corresponding to the TO-like mode of the Ge matrix and the other due to the Si—Ge bonds. Their frequencies increase with x. For $x>0.9$, the Ge—Ge bond peak becomes quite strong and a very strongly localized mode appears at 370 cm^{-1} due to a Si atom sitting in the cage of Ge atoms.

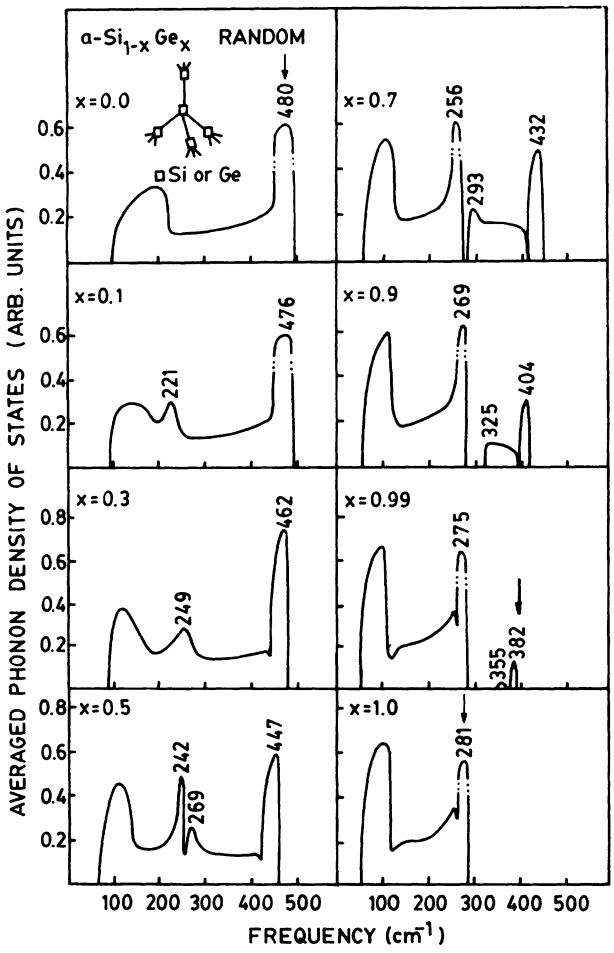

FIG. 1. Local phonon density of states (DOS) for different concentrations of constituent atoms for random a-$Si_{1-x}Ge_x$ alloys. Arrows indicate the locations of experimental peaks (Ref. 13).

The Raman data of Lannin[13] and of Tsuda *et al.*[6] for a-$Si_{1-x}Ge_x$ alloys reveal two peaks corresponding to the Ge—Ge and Si—Si bonds at 290 and 480 cm^{-1}, respectively, and an extra peak near 400 cm^{-1}. Thus, in an a-$Si_{1-x}Ge_x$ alloy, one may always envisage the occurrence of some clusters of Ge atoms surrounding a Si atom irrespective of the value of x. The results of another calculation performed for the chemically ordered $Si_{1-x}Ge_x$ alloys where one Si (Ge) atom is sitting in the cage of Ge (Si) atoms are shown in Fig. 2. One observes a localized mode near 370 cm^{-1} for the concentration range $0.4<x<0.99$. This feature is in conformity with the experimental data.[6,13]

B. a-Ge_xSi_{1-x}:H alloys

The force constants for the various bonds in these alloys have been taken over from these used earlier[14,15] for

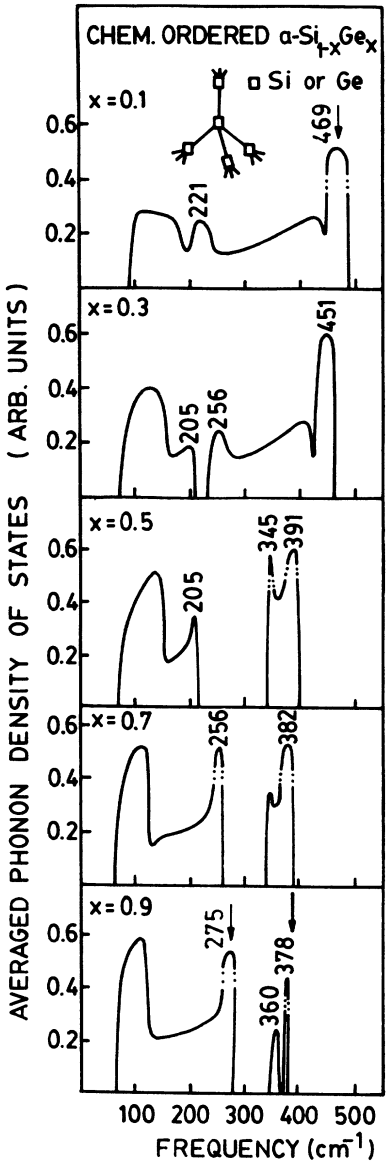

FIG. 2. Local phonon DOS for chemically ordered a-$Si_{1-x}Ge_x$ alloys. Arrows indicate the locations of experimental peaks (Ref. 13).

TABLE I. Values of the force constants (in units of 10^4 dyn/cm).

Unit	Central α (Si—X)	Angular K_1(Si—Si—X)	K_3(X—Si—X)
Si—H	22.7	0.90	
Si—H_2	24.8	1.59	1.68
Si—F	44.3	1.20	
Si—F_2	54.0	1.20	3.00
	α(Si—Si)=11.6		
	β(Si—Si)=2.0		
Unit	Central α(Ge—X)	Angular K_1(Ge—Ge—X)	K_3(X—Ge—X)
Ge—H	20.5	0.72	
Ge—H_2	23.2	0.72	1.56
Ge—F	40.0	0.96	
Ge—F_2	48.8	0.96	2.4
	α(Ge—Ge)=10.6		
	β(Ge—Ge)=1.4		
	K(Si—Si—Si)=K(Ge—Ge—Ge)=0.10		

the pure a-Si:H and the a-Ge:H alloys. The value for the angle bending force constant K(H—Si—Ge) or K(H—Ge—Si) involving both the Si and Ge atoms is taken to be equal to the corresponding value of K(H—Si—Si) or K(H—Ge—Ge) obtained earlier in the pure Si or Ge alloys. They are presented in Table I. The results for the local phonon density both at Si and H atoms for SiH_n and GeH_n ($n=1,2$) complexes in a-Ge_xSi_{1-x} alloys are shown in Figs. 3–6.

1. *Monohydrides (SiH and GeH)*

a. SiH complex. For a single H atom coupled to a Si atom (SiH) in Ge_xSi_{1-x} alloys (see Fig. 3), the bond stretching and the bond bending frequencies of the Si—H bond appearing at 2000 and 630 cm^{-1} in pure a-Si remain unaffected by the presence of the Ge atoms lying in the nearest-neighboring sites of the reference Si atoms. The results are in good agreement with the infrared[5] and Raman[6] data available for $Si_{0.53}Ge_{0.47}H$ and $Si_{0.4}Ge_{0.6}$:H alloys, respectively. The measured H-induced peaks appearing at 2022, 622, 459, 365, and 260 cm^{-1} are quite close to the calculated ones.

The light mass of the H atom is expected to affect the phonon density in a manner very much similar to that of

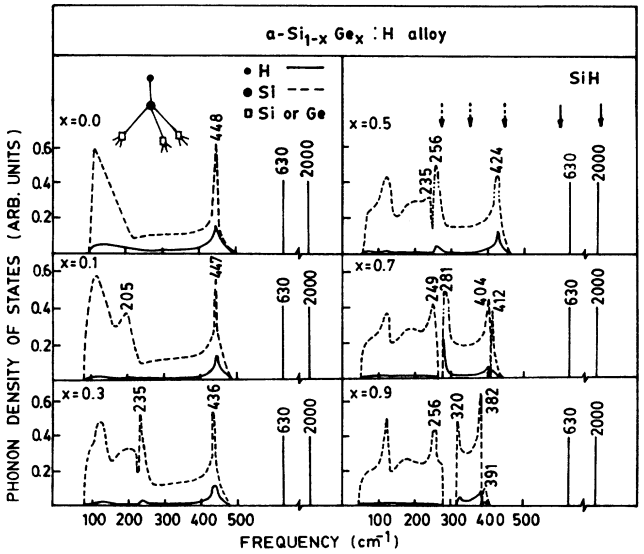

FIG. 3. Local phonon DOS at Si (— — —) and H (——) atoms for monohydride (SiH) in a-$Si_{1-x}Ge_x$ alloys. Continuous and dashed arrows indicate the experimental peaks from Refs. 5 and 6, respectively.

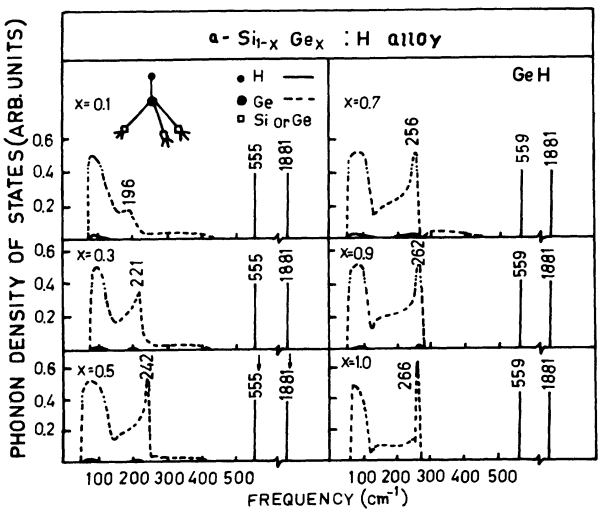

FIG. 4. Local phonon DOS at Ge (— — —) and H (——) atoms for GeH in a-$Si_{1-x}Ge_x$ alloys. Arrows indicate the experimental peaks from Ref. 5.

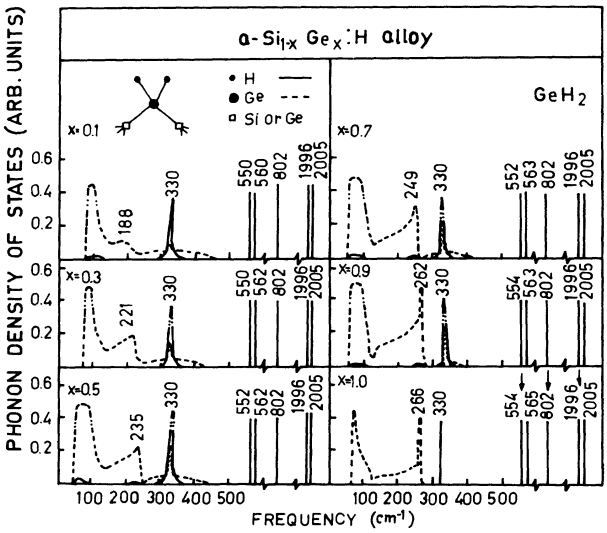

FIG. 6. Local phonon DOS at Ge (— — —) and H (——) atoms for GeH_2 in a-$Si_{1-x}Ge_x$ alloys. Arrows indicate the experimental peaks for pure a-Ge:H (Ref. 16).

a dangling bond. The states near the top of the phonon band are shifted to the low-frequency side, peaking around 125 cm^{-1}.

b. GeH complex. For the case of a H atom coupled to a Ge atom (see Fig. 4) (GeH), the behavior is very much similar to that of the SiH complex. The Ge—H bond-stretching frequency at 1881 cm^{-1} seen earlier in pure a-Ge:H alloys remains unaltered. Similarly, the Ge-H wagging mode at 556 cm^{-1} remains unaltered for the entire concentration range of x. Again, similarly to the SiH complex, enhancement in the local phonon density appears in the low-frequency region. The Si-H and Ge-H stretching and wagging vibrational modes observed in the a-$Si_{0.53}Ge_{0.47}$:H alloys by infrared absorption measurements[4–6] are in good agreement with the calculated results.

2. *Dihydrides (SiH_2 and GeH_2)*

The values for the angle bending force cosntants K_1(Si—Si—H) or K_1(Ge—Ge—H) and for K_3 (H—Si—

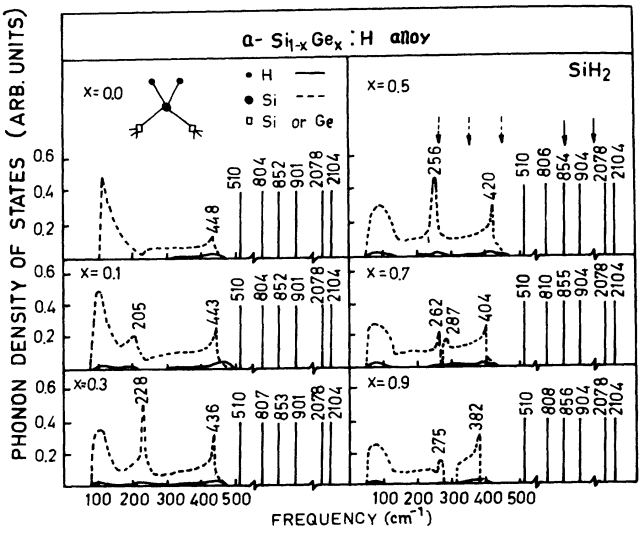

FIG. 5. Local phonon DOS at Si (— — —) and H (——) atoms for dihydride (SiH_2) in a-$Si_{1-x}Ge_x$ alloys. Continuous and dashed arrows indicate the experimental peaks from Refs. 5 and 6, respectively.

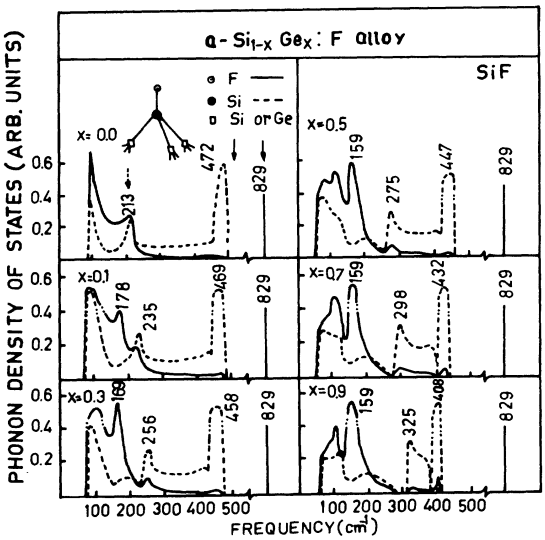

FIG. 7. Local phonon DOS at Si (— — —) and F (——) atoms for monofluoride SiF in a-$Si_{1-x}Ge_x$ alloys. Continuous and dashed arrows indicate the experimental peaks from Refs. 17 and 18, respectively.

H) or K_3 (H—Ge—H) chosen earlier to reproduce the experimentally observed doublets at 845 and 890 cm^{-1} and 862 and 907 cm^{-1} in pure a-Si:H alloys are used here. However, the corresponding doublets in a-Ge:H have not been reported in any measurement made so far.

The local phonon density at Si and H atoms for the SiH_2 unit in a-Ge_xSi_{1-x} alloys for $0.1 \leq x \leq 0.9$ is shown in Fig. 5. The H-induced high-frequency localized modes lying outside the bulk phonon bands remain almost unaffected.

Paul[4] and Rudder *et al.*[5] have detected peaks in the infrared data corresponding to the stretching and wagging vibrations of the isolated dihydrides or interacting dihydrides in a-$Si_{0.53}Ge_{0.47}$:H alloys. The locations of the experimental peaks at 2022 and 867 cm^{-1} are in good agreement with the calculated ones.

The phonon density increases further in the low-frequency region, a behavior similar to a silicon atom containing two dangling bonds.

For the GeH_2 unit the results have been presented in Fig. 6. Again practically no or very small changes are seen to occur in the locations of all six H-induced peaks.

3. a-$Si_{1-x}Ge_x$:F alloys

a. Monofluorides (SiF and GeF). The local phonon density for the monofluorides in a-Ge_xSi_{1-x} alloys in the entire concentration range ($0.1 \leq x \leq 0.9$) is presented in Figs. 7 and 8. The Si—F (Ge—F) bond-stretching frequency at 829 (677) cm^{-1} remains undisturbed by the relative concentrations of the two types of constituent atoms present in the alloy. However, the inband wagging and/or bending vibrations show appreciable variation in frequency with x. For SiF, the inband wagging mode frequency changes from 213 to 159 cm^{-1} whereas for GeF it varies from 159 to 142 cm^{-1}.

b. Difluorides (SiF_2 and GeF_2). The calculated results for the local phonon density at the different atoms for the difluorides are presented in Figs. 9 and 10. For the SiF_2 configuration (Fig. 9), the asymmetric and symmetric stretching vibrations appearing at 968 and 862 cm^{-1}, re-

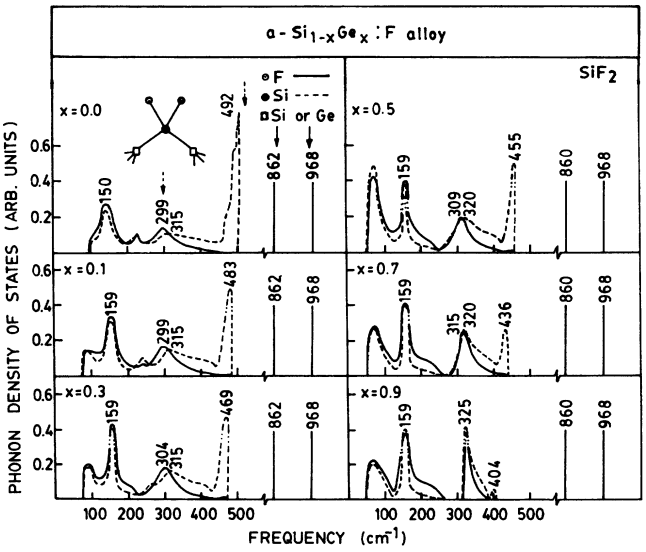

FIG. 9. Local phonon DOS at Si (— — —) and F (——) atoms for difluoride (SiF_2) in a-$Si_{1-x}Ge_x$ alloys. Continuous and dashed arrows indicate the experimental peaks from Refs. 19 and 16, respectively.

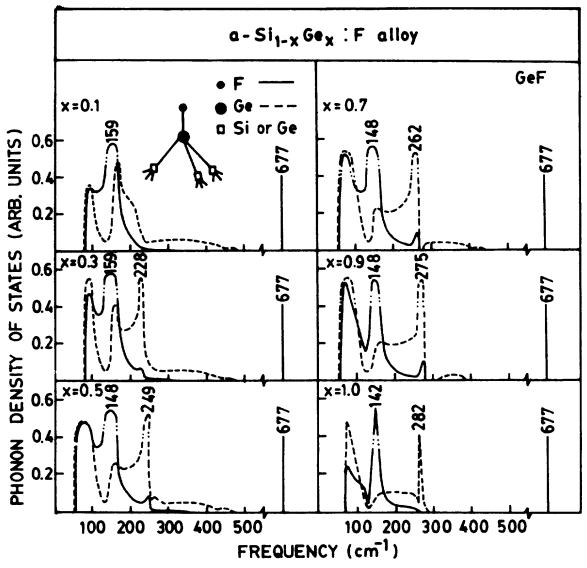

FIG. 8. Local phonon DOS at Ge (— — —) and F (——) atoms for GeF in a-$Si_{1-x}Ge_x$ alloys.

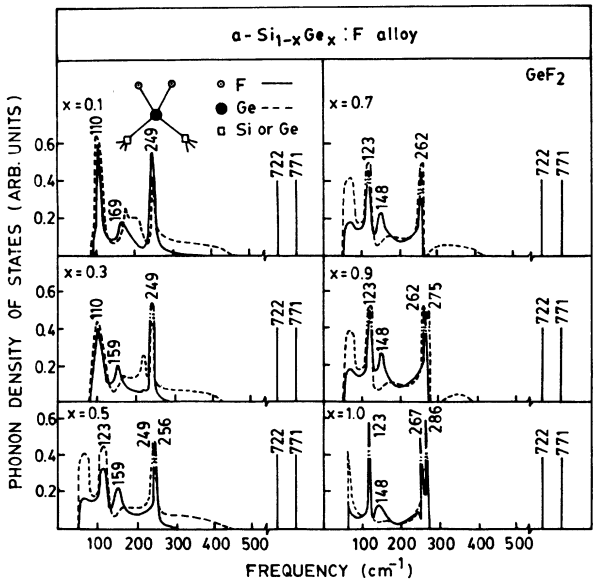

FIG. 10. Local phonon DOS at Ge (— — —) and F (——) atoms for GeF_2 in a-$Si_{1-x}Ge_x$ alloys.

TABLE II. Values of the force constants.

System	Force constants 10^4 dyn/cm) Central (α)	Noncentral (β)
Ga-As	10.8	1.0
Al-As	11.3	1.0

spectively, lying outside the bulk phonon bands remain unaffected by the presence of Ge atoms. Also, the F-induced peak at 159 cm^{-1} in the bulk phonon region remains undisturbed by the relative concentratoins of Si and Ge atoms. On the other hand, another F-induced peak shows an appreciable variation in frequency, i.e., from 300 to 325 cm^{-1} with x.

For the GeF_2 complex (Fig. 10), again the asymmetric and symmetric stretching modes remain unaffected by the presence of Si atoms. However, the two F-induced in-band modes show variations in their frequencies, i.e., from 110 to 123 cm^{-1} and from 169 to 148 cm^{-1} with x.

IV. $Ga_{1-x}Al_xAs$ ALLOYS

The force constant parameters, i.e., the radial (α) and the nonradial (β) ones for the end components GaAs and AlAs have been adjusted to reproduce the experimentally observed maximum frequencies (see Table II). The computed phonon density of states has been compared with the available experimental data of Sapriel *et al.*[20,21] and Ilegems and Pearson[22] in Fig. 11. The bulk phonons for the pure GaAs and AlAs have been well reproduced.

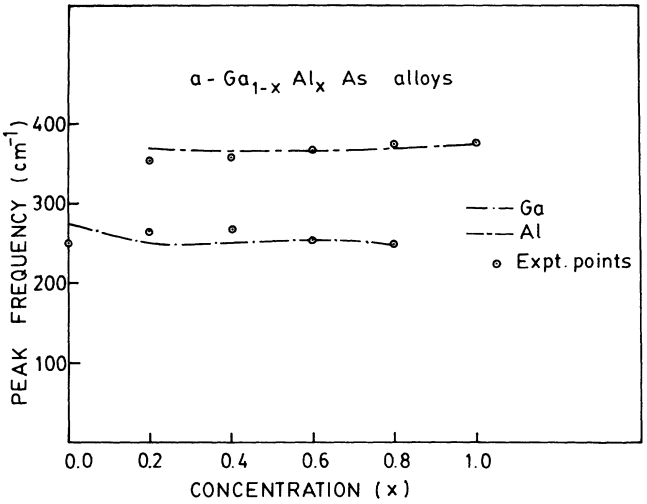

FIG. 12. Variation of peak frequencies with concentration of Al atoms (x) along with the experimental points available for mixed crystals (Ref. 23).

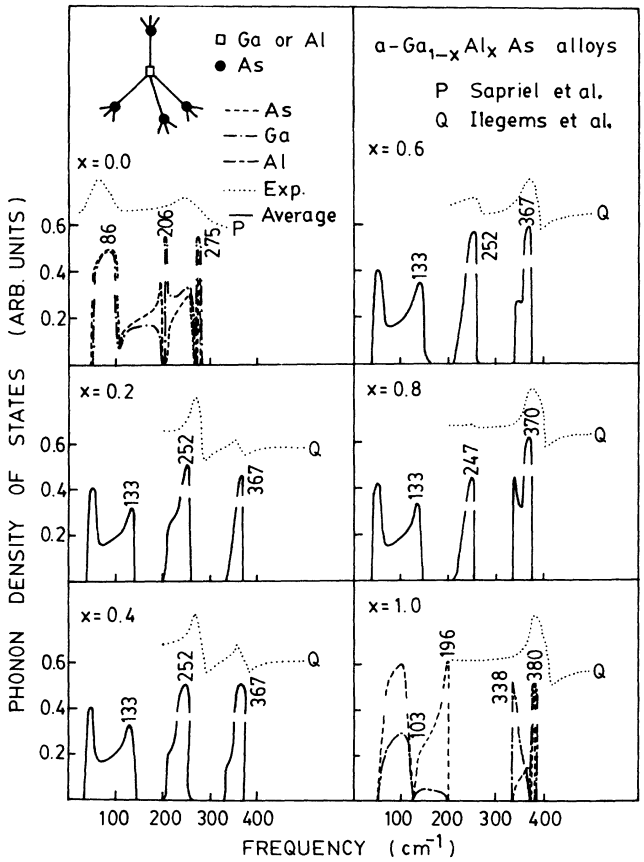

FIG. 11. Averaged local phonon DOS in a-$Ga_{1-x}Al_xAs$ alloys for different concentrations (x) of Al atoms. Dotted curves are the Raman data of Sapriel *et al.* (Ref. 21) and the reflectivity data of Ilegems and Pearson (Ref. 22).

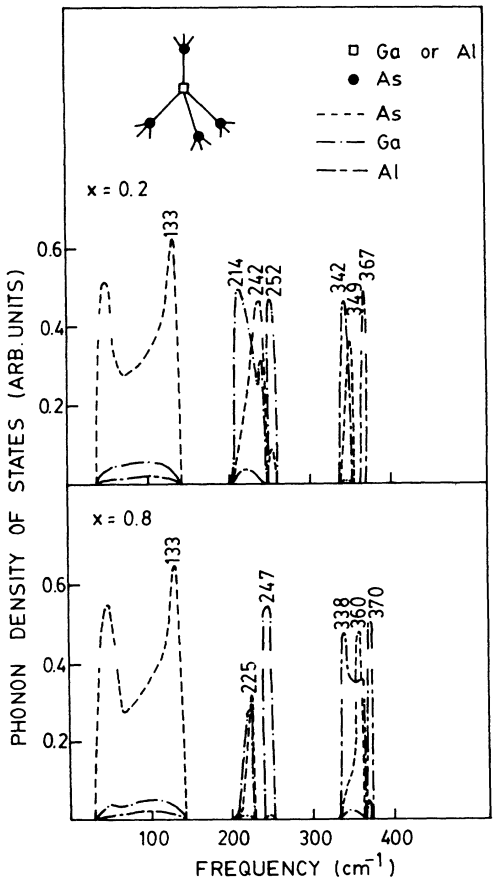

FIG. 13. Local phonon DOS on Ga, As, and Al atoms for a-$Ga_{1-x}Al_xAs$ alloys for $x=0.2$ and 0.8.

The calculated local phonon density of states at all three kinds of atoms, Ga, Al, and As, for different concentrations x, is presented in Fig. 11. The available reflectivity data of Ilegems and Pearson[22] in the optical mode region and the Raman data of Kim and Spitzer[23] and Saint-Cricq *et al.*[24] for mixed cyrstals compare very well with the features arising from the transverse-optic modes in the averaged density of states calculated for a random distribution of Ga and Al atoms in the $Ga_{1-x}Al_xAs$ alloys. The variation of the optical mode frequencies with the concentration x of Al atoms, along with the experimental values, is shown in Fig. 12.

The local density of states on the three kinds of atoms, Ga, As, and Al, for concentrations $x=0.2$ and 0.8, is shown in Fig. 13. For $x=0.2$, at the As atom which is the heaviest of all, peaks mainly appear near 133 and 242 cm^{-1}. For the Ga atom, peaks are seen at 214 and 252 cm^{-1}, whereas for the light Al atom one observes structures only in the high-frequency region near 367 cm^{-1}. Similar arguments are valid for $x=0.8$.

V. CONCLUSIONS

In the present comprehensive study of the vibrational excitations of the hydrogenated and/or fluorinated amorphous silicon-germanium alloys, we find that the H- (F-) induced localized vibrational modes lying outside the bulk silicon-germanium phonon band region remain unaltered by the presence of the other kind of host atoms. However, a number of low-frequency inband modes incurred by F atoms change their locations with the reltaive concentrations of the constituent Si and Ge atoms. But these changes lie well within $\sim 10\%$. The calculated results are in good agreement with the available experimental data. However, a number of the predicted modes lying mainly in the bulk phonon band region have not been detected so far. More careful and detailed experimental investigations are very much needed to improve the present situation.

In a-$Ga_{1-x}Al_xAs$ alloys, a random microscopic arrangement of the Ga and Al atoms is seen to explain the available experimental data well.

ACKNOWLEDGMENTS

The authors express their thanks to Department of Science and Technology, Government of India (New Delhi) and to the University Grants Commission, Government of India (New Delhi), for financial assistance.

[1]Y. Kuwano, Tech. Dig. Int. PVSEC-1 **13**, (1984).
[2]S. Tsuda, N. Nakamura *et al.*, Jpn. J. Appl. Phys. **21**, Suppl. 21-2, 251 (1982).
[3]For numerous papers, see J. Non-Cryst. Solids **77&78**, (1985).
[4]W. Paul, in *Fundamental Physics of Amorphous Semiconductors,* edited by F. Yonezawa (Springer-Verlag, New York, 1981), p. 72.
[5]R. A. Rudder, J. W. Cook, and G. Lucovsky, in *Proceedings of the 17th International Conference on Physics of Semiconductors,* edited by J. D. Chadi and W. A. Harrison (Springer-Verlag, New York, 1985), p. 901.
[6]S. Tsuda, H. Tarui, H. Haku, Y. Nakashima, Y. Hishikawa, S. Nakano, and Y. Kuwano, J. Non-Cryst. Solids **77&78**, 845 (1985).
[7]F. Yndurain, Phys. Rev. B **18**, 2876 (1978).
[8]R. C. Kittler and L. M. Falicov, J. Phys. C **9**, 4259 (1976).
[9]Bal K. Agrawal, Phys. Rev. B **22**, 6294 (1980); Solid State Commun. **37**, 271 (1981); Phys. Rev. B **26**, 5972 (1982).
[10]R. Barrio, R. J. Elliott, and M. F. Thorpe, J. Phys. C **15**, 4493 (1983).
[11]Bal K. Agrawal and Savitri Agrawal, Phys. Rev. B **36**, 2799 (1987).
[12]S. Adachi, J. Appl. Phys. **58**, R1 (1985).
[13]J. S. Lannin, Phys. Rev. B **16**, 1510 (1977).
[14]Bal K. Agrawal and B. K. Ghosh, J. Phys. C **18**, 3897 (1985); J. Non-Cryst. Solids **77&78**, 1105 (1985).
[15]B. K. Ghosh and Bal K. Agrawal, Phys. Rev. B **33**, 1250 (1986).
[16]G. Lucovsky, S. S. Chao, J. Yang, J. E. Tyler, R. C. Ross, and W. Czybatyi, Phys. Rev. B **31**, 2190 (1985).
[17]C. J. Fang, L. Ley, H. R. Shanks, K. J. Grunta, and M. Cardona, Phys. Rev. B **22**, 6140 (1980).
[18]S. C. Shen, C. J. Fang, and M. Cardona, Phys. Status Solidi B **101**, 451 (1980).
[19]T. Shimada, Y. Katayama, and S. Horigome, J. Appl. Phys. **19**, L265 (1980).
[20]J. Sapriel, J. C. Michel, J. C. Toledano, and R. Vacher, J. Phys. (Paris) Colloq. **C5**, 139 (1984).
[21]J. Sapriel, Y. I. Nissim, B. Joukoff, J. L. Oudar, S. Abraham, and R. Beserman, J. Phys. (Paris) Colloq. **C5**, 75 (1984).
[22]M. Ilegems and G. L. Pearson, Phys. Rev. B **1**, 1576 (1970).
[23]O. K. Kim and W. G. Spitzer, J. Appl. Phys. **50**, 4362 (1979).
[24]N. Saint-Cricq, R. Carles, J. B. Renucci, A. Zwick, and M. A. Renucci, Solid State Commun. **39**, 1137 (1981).